Published in final edited form as:
Oncogene. 2013 January 17; 32(3): 286–295. doi:10.1038/onc.2012.46.

Protein Kinase C iota as a Therapeutic Target in Alveolar Rhabdomyosarcoma

Ken Kikuchi[1], **Anuradha Soundararajan**[2], **Lee Ann Zarzabal**[3], **Capella R. Weems**[4], **Laura D. Nelon**[2], **Sheila T. Hampton**[2], **Joel A. Michalek**[3], **Brian P. Rubin**[5], **Alan P. Fields**[4], and **Charles Keller**[1,*]

[1]Pediatric Cancer Biology Program, Pape' Family Pediatric Research Institute, Department of Pediatrics, Oregon Health & Science University, Portland, OR

[2]Greehey Children's Cancer Research Institute, University of Texas Health Science Center, San Antonio, TX

[3]Departments of Epidemiology and Biostatistics, University of Texas Health Science Center, San Antonio, TX

[4]Department of Cancer Biology, Mayo Clinic Comprehensive Cancer Center, Jacksonville, FL

[5]Departments of Anatomic Pathology and Molecular Genetics, Cleveland Clinic, Taussig Cancer Center and the Lerner Research Institute, Cleveland, OH

Abstract

Alveolar rhabdomyosarcoma is an aggressive pediatric cancer exhibiting skeletal muscle differentiation. New therapeutic targets are required to improve the dismal prognosis for invasive or metastatic alveolar rhabdomyosarcoma. Protein kinase C iota (PKCι) has been shown to play an important role in tumorigenesis of many cancers but little is known about its role in rhabdomyosarcoma. Our gene expression studies in human tumor samples revealed overexpression of *PRKCI*. We confirmed overexpression of PKCι at the mRNA and protein level using our conditional mouse model that authentically recapitulates the progression of rhabdomyosarcoma in humans. Inhibition of *Prkci* by RNA interference resulted in a dramatic decrease in anchorage-independent colony formation. Interestingly, treatment of primary cell cultures using aurothiomalate (ATM), which is a gold-containing classical anti-rheumatic agent and a PKCι-specific inhibitor, resulted in decreased interaction between PKCι and Par6, decreased Rac1 activity and reduced cell viability at clinically relevant concentrations. Moreover, co-treatment with ATM and vincristine, a microtubule inhibitor currently used in rhabdomyosarcoma treatment regimens, resulted in a combination index (C. I.) of 0.470–0.793 through cooperative accumulation of non-proliferative multinuclear cells in the G2/M phase, indicating that these two drugs synergize. For *in vivo* tumor growth inhibition studies, ATM demonstrated a trend towards enhanced vincristine sensitivity. Overall, these results suggest that PKCι is functionally important in alveolar rhabdomyosarcoma anchorage-independent growth and tumor cell proliferation and that combination therapy with ATM and microtubule inhibitors holds promise for the treatment of alveolar rhabdomyosarcoma.

[*]Corresponding author: Pediatric Cancer Biology Program, Pape' Family Pediatric Research Institute, Department of Pediatrics, Oregon Health & Science University, 3181 S.W. Sam Jackson Park Road, Mail Code: L321, Portland, OR 97239-3098, Tel 503.494.1210, Fax 503.418.5044, keller@ohsu.edu.

Conflict of interest
The authors declare no conflict of interest.

Keywords

Alveolar rhabdomyosarcoma; protein kinase C iota; Rac1; mitosis; aurothiomalate; vincristine

Introduction

Rhabdomyosarcoma (RMS) is a group of aggressive muscle cancers and the most common soft tissue sarcomas in children and adolescents (1). RMS can arise from skeletal muscle and non-muscle tissues in the body and the prognosis is dependent on the site of origin and histological subtype (2). Alveolar (ARMS) and embryonal (ERMS) are the two major subtypes of RMS in children and adolescents and have distinct genetic abnormalities and biological behavior (3). ARMS accounts for 25% of all RMS and are accompanied by a high frequency of invasion and metastasis at the time of initial diagnosis. Despite a multidisciplinary approach, including surgical resection, irradiation, and intensive chemotherapy, many children with invasive or metastatic ARMS die of their disease (4). Target discovery is ongoing to develop molecularly targeted therapies with the goal of improving prognosis (5).

Protein Kinase C (PKC) is a family of serine/threonine kinases made up of at least 12 isozymes (6). PKC isozymes play crucial roles in diverse cellular signaling processes including cellular proliferation, differentiation, apoptosis and angiogenesis (7). PKC isozymes are classified into three major categories as classic (α, βI, βII, and γ), novel (δ, ε, η, and θ) and atypical (ξ and ι/λ). Biochemical and immunologic studies indicate that multiple PKC isozymes are expressed in virtually all cell and tissue types (8). The expression of individual PKC isozymes is developmentally regulated and is responsive to the differentiation state of cells and tissues. The role of PKC isozymes in tumor biology is dependent on the cell type and intracellular localization and hence the different isozymes may have opposing effects in the same cell (9). PKC isozymes have not only been implicated in the pathogenesis of many cancers including breast, colon, lung, prostate, pancreatic, liver and hematopoietic system (8, 9) but also in the development of multidrug resistance (9–12).

Although PKC isozyme expression varies in different cancers, only PKC iota (PKCι) has been shown to be a human oncogene (13, 14). PKCι plays a pivotal role in the tumorigenesis of lung, pancreatic, prostate, colon, and ovarian cancers (15–24). Recent findings suggested that this transformation can be prevented both *in vitro* and *in vivo* using a gold-containing classical anti-rheumatic agent, aurothiomalate (ATM). ATM disrupts the interaction between the PB1 domain of PKCι and Par6 (13, 18, 24, 25), a protein involved in the polarity complex formation (26), and inhibits Rac1 activity which is a critical downstream effector of oncogenic PKCι (27).

Phosphorylation profiles in human ARMS and ERMS indicate that phosphorylation levels of PKCα, δ, θ, and ξ are upregulated and hence could play roles in the development or progression of RMS (28). Although few reports are available on the expression profile of the PKC family in RMS, involvement of individual PKC isozymes and their use as therapeutic targets are beginning to be explored (8, 29, 30). Herein we report the characterization of *PKC* isozymes in RMS, with a focus on the functional role of PKCι in the alveolar subtype of RMS. Moreover, our data hold forth the possibility that ATM might be an adjuvant therapy for use in combination with standard rhabdomyosarcoma chemotherapy.

Results

PKCι is over-expressed in human rhabdomyosarcoma

Expression of *PKC* isoforms in RMS was determined using real time reverse transcription (RT)-PCR amongst human skeletal muscle, ARMS and ERMS samples. A full profile is shown in Supplemental Figure S1. Among the isozymes, only *PRKCI* and *PKCμ* were differentially increased in RMS tumors. Both ARMS and ERMS expressed *PRKCI* at 2–4 orders of magnitude higher than normal skeletal muscle ($p<0.05$) (Figure 1a). To determine if the over-expression of *PRKCI* was due to genomic amplification, the gene copy number of *PRKCI* in human ARMS DNA was compared to that in cases of lung squamous cell carcinoma harboring *PRKCI* amplification. No genomic amplification of *PRKCI* was observed in the examined cohort of *PRKCI* over-expressing ARMS (Figure 1b). To confirm that over-expression of *PRKCI* mRNA translated into over-expression of PKCι at the protein level, immunohistochemistry was performed on human ARMS and ERMS specimens ($n = 40$ and $n = 5$, respectively). Alveolar rhabdomyosarcoma tumors in particular demonstrated PKCι expression in greater than 50% of cells for 77.5% of cases, whereas normal skeletal muscle rarely expressed strong PKCι (Figure 1c). Thus, PKCι mRNA and protein is overexpressed in human ARMS and ERMS. PKCι was expressed in tumor cells but not in non-neoplastic cells in the tumor microenvironment.

PKCι is over-expressed in a rhabdomyosarcoma mouse model

To validate that our mouse models of ARMS and ERMS reflect the characteristics of human RMS tumors, expression of *Prkci* in murine ARMS or ERMS was compared to normal mouse skeletal muscle using real time RT-PCR (Figure 2a). As seen in human RMS, mouse ARMS and ERMS over-expressed *Prkci* to a level 7- to 35-fold higher than normal mouse skeletal muscle. Immunohistochemistry on paired mouse skeletal muscle and RMS tumor samples indicated consistently strong *Prkci* expression levels in tumors as compared to skeletal muscle (representative results are shown in Figure 2c). We next focused on ARMS, given the particularly poor prognostic outcomes seen in the clinic (4). To demonstrate that PKCι was not only expressed but was also activated in ARMS, immunoblotting was performed to determine expression and phosphorylation of PKCι on paired skeletal muscle and tumor samples. PKCι was over-expressed and highly activated in the primary tumors relative to normal skeletal muscle (Figure 2b). Alveolar rhabdomyosarcoma primary cell cultures (U20325, U21459 and U23674) established from biopsies taken at necropsy from mice were used to analyze the PKCι signaling axis in ARMS, *in vitro*. Mouse primary cell cultures exhibited high expression of *Prkci* at the mRNA level in comparison to a normal mouse myoblast cell line C2C12 (Figure 2d). The expression and activation of PKCι at the protein level was higher in the primary cell cultures when compared to C2C12 as confirmed by immunoblotting (Figure 2e, Supplementary Figure S2) and reflected the trend observed at the mRNA level for primary cell cultures (Figure 2a).

Suppression of PKCι inhibits mouse tumor cell colony formation *in vitro*

To confirm the role of PKCι in ARMS cells, a mouse specific *Prkci* small interfering RNA (siRNA) was transfected into mouse primary cell cultures. Immunoblotting was used to confirm depletion of PKCι. *Prkci* siRNAs at ≥1 nM depleted total PKCι and its phosphorylated form efficiently (Figure 3a, Supplementary Figure S3). Anchorage-independent colony formation was also markedly inhibited at 10–100 nM of *Prkci* siRNA (Figure 3b). In contrast, primary cell cultures transfected with *Prkci* siRNA did not show a decrease in growth when treated with 1 to 100 nM *Prkci* siRNA (Figure 3c). These results are consistent with previous findings in intestinal epithelial cells, non–small cell lung carcinoma cells, pancreatic cancer cells and ovarian cancer cells, which also showed inhibition of anchorage-independent colony formation but not growth (18, 19, 22–24).

ATM inhibits mouse tumor cell proliferation *in vitro*

In an effort to translate these studies to the clinic, ATM, a highly selective inhibitor of PKCι, was used to inhibit PKCι function in mouse ARMS primary cell cultures. ATM was identified through a high-throughput drug screen for its ability to inhibit PKCι binding to its effector, Par6, *in vitro* (24). PKCι mediated transformation requires activation of the more downstream effector molecule, Rac1. PKCι regulates Rac1 through interaction with Par6 (18). Our previous studies demonstrated that ATM is particularly effective as an anti-tumor agent in tumor cells that express elevated levels of its target PKCι (17). Given our current observation that ARMS tumors express high levels of PKCι, we hypothesized that ATM would have anti-tumor activity against ARMS. In our experiments, immunoprecipitation of PKCι and Par6 revealed that the PKCι-Par6 interaction in ARMS cell was decreased by ATM at clinically achievable concentrations in a dose-dependent manner (Figure 4a, Supplementary Figure S4). To determine if PKCι was important for invasion of tumor cells, we performed an invasion assays with primary cell cultures treated with increasing concentrations of ATM (10 to 500 μM) (Figure 4b). No statistical difference was found in the number of cells invading through the extracellular matrix chamber between untreated and treated cells expect at the high concentration of ATM (500 μM). Next, primary cell cultures were treated with increasing concentrations of ATM (10 to 1000 μM) (Figure 4a). Interestingly, the growth of primary cell cultures was inhibited to a greater degree than for C2C12, which is a mouse myoblast cell line. For ARMS primary cell cultures the IC50 ranged from 54 to 166 μM.

Treatment with VCR and ATM has synergic effect through G2 phase mediated non-proliferative multinuclear cell accumulation

We next investigated co-treatment with ATM and vincristine (VCR) because of the recently demonstrated role of Rac1 in mitosis (31–33). In a cell growth assay, ATM increased VCR sensitivity of mouse ARMS cells cooperatively, with combination index (C.I.) values lower than 1.0 at clinically relevant concentrations of 25 μM ATM (34) and 5 nM VCR (35) (Figure 5a–f). Human ARMS cell line Rh30 which also expressed PKCι phospho-PKCι and Par6, showed same tendency of ATM and VCR combination as compared with C2C12 (Supplementary Figure S5). Cell cycle analysis of the primary cell cultures treated with ATM and VCR revealed an increasing percentage of cells in the G2 phase or in cells having ≥4N DNA content with the combination of ATM and VCR as compared to ATM only or VCR only ($p<0.05$) (Figure 6a). Rac1 activation assay revealed that ATM treatment decreased Rac1 activity ($p<0.05$), whereas VCR treatment had no effect on Rac1 activity (Figure 6b). To confirm these findings, we performed immunocytochemistry for β-tubulin and DAPI with ATM and/or VCR treated cells. The number of multinuclear cells (MNC) was increased by VCR, and a statistically significant difference was found in the number of MNC between VCR alone and VCR plus ATM ($P<0.05$) (Figure 6c). Moreover, Ki67 immunofluorescence showed that the population of non-proliferative MNC was increased by ATM and VCR (71.2% vs 58.8% Ki67 positive MNC with VCR + ATM vs VCR alone) ($p<0.05$) (Figure 6c, Supplementary Figure S6). These MNC did not have activated apoptosis as measured by Cleaved Caspase-3 stain, TUNEL assay or Annexin-V/PI stains assay, cellular senescence as measured by senescence associated β-galactosidase stain, or muscle differentiation as detected by myosin heavy chain expression (Supplementary Figure S7).

ATM enhanced VCR sensitivity *in vivo*

Next we assessed the effect of combination with ATM and VCR *in vivo*. We previously showed that the serum gold level associated with a dose of ATM 60 mg/kg i.m. injection daily for mouse was consistent with the serum gold level typically observed in rheumatoid arthritis patients undergoing ATM therapy (17). VCR dose was chosen at 1 mg/kg based on

previous report (36, 37). Tumor growth exhibited a consistent trend decrease in the ATM treated group comparing control group. While VCR was able to decrease tumor growth significantly, ATM led to a consistent trend to improve VCR sensitivity *in vivo* although this trend did not reach significance (Figure 7a, Table S2a). With regard to differential toxicity, no significant differences in mice body weight between control vs ATM treated group, and VCR vs VCR and ATM treated group were observed (Figure 7b, Table S2b).

Discussion

Rhabdomyosarcomas are the most common tissue sarcomas in children. Despite efforts to improve treatment regimens, the survival rate for RMS, especially ARMS, has remained unchanged for the past two decades; the 4-year survival rate for patients with metastatic ARMS expressing PAX3-FKHR was reported to be 20% or less (2, 3, 38). These poor clinical outcomes have fueled the need for a better understanding of the tumorigenic mechanisms so that new therapeutic targets/opportunities can be identified (5). Recently, PKCι had been identified as an oncogene in non-small cell lung cancer (14). Over-expression of PKCι has been linked to progression and metastases of many cancers such as lung, prostate, pancreatic, colon, esophageal, liver, breast, ovarian and brain tumor (8, 27). In this report, we conducted the first known study to determine the role of PKCι in ARMS tumorigenesis and explore its potential as a therapeutic target in this disease. To establish the relevance of PKCι in RMS tumorigenesis, we first confirmed that PKCι is over-expressed in human RMS versus normal skeletal muscle. While over-expression of *PRKCI* mRNA is attributable to tumor specific gene amplification of *PRKCI* in squamous cell carcinomas of lung (14), we found no genomic amplification of *PRKCI* in the RMS samples we tested, though examination of a larger cohort of human tumors may be warranted. We have also shown that PKCι protein over-expression parallels its mRNA over-expression in human tumors. We validated that our conditional mouse ARMS model had the same characteristics as human ARMS in terms of PKCι over-expression at the mRNA and protein level and thus could be used to study the role of PKCι in ARMS tumorigenesis.

While our work is the first to examine the role of PKCι in ARMS, a role for other PKC isoforms in RMS is also emerging. Many of these studies result from the ability of the broad spectrum PKC activating compound 12-Otetradecanoyl-Phorbol-13-acetate (TPA) to induce differentiation in ERMS and ARMS cell lines (39–41). More specific reports have demonstrated that PKCα, PKCδ, PKCθ, and PKCζ may be phosphorylated in approximately two-thirds of ARMS and half of ERMS (28). One therapeutically-based study has gone so far as to suggest that PKC isoforms may be required for phosphorylation and activation of the Pax3:Fkhr chimeric transcription factor in ARMS (29). Another study indicated that PKCμ and PKCε (and perhaps PKCθ) are mediators of Igf-1 protection against rapamycin-induced apoptosis in a Pax3:Fkhr expressing ARMS (42). Meanwhile, other studies are focused on the roles of PKC isoforms upstream or downstream of cell surface interacting proteins. For example, in an ERMS cell line, PKCε was suggested to play a role in cell surface localization of microenvironment interacting metalloproteases (43), whereas PKCζ was thought to play a role downstream in the response to IL-1beta (44).

Recently we and others have shown that PKCι drives anchorage-independent growth of lung, colon and ovarian cancers (14, 18, 22, 23). Using RNA interference, we have now established that PKCι also plays a role in ARMS transformation as measured by anchorage-independent growth. Genetic inhibition of *Prkci* reduced the relative number of colonies formed by ARMS primary cell cultures but had no effect on a normal mouse myoblast cell line. We evaluated PKCι as a therapeutic target using the selective PKCι inhibitor ATM, a therapeutic agent we recently discovered and have taken into clinical trials for lung cancer (Clinicaltrials.gov, NCT 00575393). ATM reduced not only the interaction of PKCι-Par6,

but also proliferation of mouse ARMS cells. ATM trough concentrations observed during ATM treatment of rheumatoid arthritis patients is 15.4–25.4 μM (34), which is slightly higher than the IC50 for our mouse ARMS cells. We next investigated the synergic effect of ATM and VCR, which binds to tubulin and inhibits microtubule formation, therefore, arresting the cell at metaphase by disrupting formation of the mitotic spindle (45). Interestingly, ATM enhanced VCR sensitivity of mouse ARMS cells and their C.I is below 1 at clinically achievable concentrations, indicating that ATM synergizes with VCR. For example, C.I.'s of 25 μM ATM and 5 nM VCR for U23674, U21459 and U20325 were 0.793, 0.572 and 0.470, respectively. Moreover, we obtained comparable results from *in vivo* experiments. Cell cycle analysis indicated that the combination of ATM and VCR induced significantly more G2 and ≥4N cells compared to VCR alone. Immunofluorescence indicated that the combination of ATM and VCR induced significantly more Ki67-negative MNC compared to VCR alone. It has been previously shown that MNC arising after VCR are incapable of proliferation and do not contribute to tumor re-growth (46). Moreover, Rac1 is a major downstream effector of PKCι-Par6 signaling axis that is inhibited by ATM (27) and known as a regulator of mitosis (31–33). In our study, Rac1 activity was reduced by ATM but not by VCR. Based on these results, we hypothesize that treatment with VCR and ATM synergize through G2 phase mediated non-proliferative and multinuclear cell accumulation (Figure 6d). We conclude that combination therapy with VCR and ATM should be investigated further for the clinical treatment ARMS and that especially for children with vincristine-associated peripheral neuropathy, adding ATM might be an approach to improve efficacy despite vincristine dose reduction. Furthermore, the greatest therapeutic value of a well-tolerated agent such as ATM may be in combination with other targeted therapeutics, which is an avenue of ongoing investigation.

Materials and Methods

Mice

All animal procedures were conducted in accordance with the Guidelines for the Care and Use of Laboratory Animals and were approved by the Institutional Animal Care and Use Committee (IACUC) at the University of Texas Health Science Center at San Antonio (UTHSCSA) and the Oregon Health & Science University (OHSU). The *Myf6Cre, Pax3:Fkhr, p53* conditional mouse model of ARMS has been described previously (47–49). The *Pax7CreER, Ptch1, p53* conditional model of ERMS is described in Rubin *et al* (50).

Human tissue samples

Human samples were obtained from the Pediatric Cooperative Human Tissue Network (Columbus, OH) with approval from the UTHSCSA and OHSU institutional review boards.

Primary tumor cell cultures and cell lines

Mouse primary cell cultures (U20325, U21459, and U23674) were established from tumor samples. Tumors were minced into small pieces and digested with collagenase (10 mg/ml) overnight at 37°C. The dissociated cells were then incubated in Dulbecco's modified eagle's media supplemented with 10% fetal bovine serum (FBS) and 1% penicillin-streptomycin in 5% CO2 at 37°C. C2C12 mouse myoblast and Rh30 human ARMS cell line were purchased from ATCC (Manassas, VA) and maintained in the same culture conditions as primary tumor cell cultures.

Quantitative PCR analysis for *PRKCI* gene amplification

Genomic DNA from each human tumor was analyzed for *PRKCI* gene amplification using Taqman technology on an Applied Biosystems 7900HT sequence detection system. The

human RNaseP1 gene was used as a DNA template control and for normalization of results. The primer/probe set for the human *PRKCI* gene was forward primer, 5′-GGCTGCATTCTTGCTTTCAGA-3′; reverse primer, 5′-CCAAAATATGAAGCCCAGTAATCA-3′; and probe, 5′-CAATCTTACCTGCTTTCT-3′. The primer/probe set for RNaseP1 gene was designed and provided by ABI Assay on Demand. A tumor was scored positive for *PRKCI* gene amplification when analysis revealed a minimum of one extra copy of the *PRKCI* allele.

Gene expression analysis

Total RNA was isolated from tumors using Trizol (Invitrogen, Carlsbad, CA) according to the manufacturer's protocol. RNA was then purified using Qiagen RNeasy miniprep cleanup kit (Qiagen, Valencia, CA). Single-stranded cDNA was generated from total RNA using first strand synthesis kit (Fermentas, Hanover, MD). Real-time PCR was performed using SYBR green PCR Master Mix (Applied Biosystems, Foster City, CA) on an ABI Prism 7500HT sequence detection system. Primers used were as follows : Human *PRKCI* (5′-TACGGCCAGGAGATACAACC-3′ and 5′-TCGGAGCTCCCAACAATATC-3′) and mouse *Prkci* (5′-GCAGATCCGCATCCCGCGTT-3′ and 5′-AATGCTGTGGGGGCTGGTGC-3′).

Histology and immunohistochemistry

Mouse tumor samples were fixed in 10% buffered formalin and embedded in paraffin. Paraffin sections (3.5 μm) were stained with hematoxylin and eosin (H&E). Immunohistochemistry was performed on paraffin sections using manufacturer's protocol using rabbit anti-PKCι antibody (cat. ab5282, Abcam, Cambridge, MA).

Immunoprecipitation and Immunoblotting

Tumors were lysed in radioimmunoprecipitation assay (RIPA) buffer or NP40 buffer containing both protease and phosphatase inhibitor (Sigma Aldrich, St. Louis, MI). The lysates were homogenized and centrifuged at 8000g for 10 minutes. The resulting supernatants were used for immunoblot analysis. Mouse monoclonal anti-PKCι antibody (cat. 610175; BD biosciences, Franklin Lakes, NJ), rabbit anti-phospho-PKCι antibody (cat. ab5813; Abcam, Cambridge, MA), rabbit anti-Par6 antibody (cat. Ab45394; Abcam, Cambridge, MA), rabbit anti-caspase-3 antibody (cat. 9662; Cell signaling Technology). Full-length blots are represented in Supplemental Figure S2–4.

Immunofluorescence stain

Cells were plated on 8-well CultureSlides (cat. 354118; BD Falcon, Franklin Lakes, NJ), fixed with 4% paraformaldehyde, permeabilized with 0.1% TritonX100, washed and incubated with mouse monoclonal anti-β-tubulin antibody (cat. E7; Developmental Studies Hybridoma Bank) and rabbit anti-Ki67 antibody (cat. RM-9106-F; Thermo scientific) overnight, rinsed with PBS, incubated with fluorescein isothiocyanate-conjugated anti-mouse and rabbit IgG (1:200) for 1 h, and examined under an inverted fluorescence microscope. Single photomontages of merged image are presented in Supplemental Figure S6.

Rac1 assay

Mouse RMS primary cell cultures were plated at 6×10^4 cells per well in a 6 well plate. After 24 h, ATM and VCR were added to the dish, after 24 h, cells were harvested and Rac1 activity was analyzed by using Rac1 G-LISA™ Activation Assay (luminescence) (cat. BK126; Cytoskeleton, Inc. Denver, CO).

Cell cycle analysis

Mouse RMS primary cell cultures were plated at 3×10^5 cells per 60 mm dish. After 24 h, ATM and VCR were added to the dish. After 24 h, cells were harvested, fixed with 70% cold ethanol, washed once in PBS, resuspended in 50 mg/ml propidium iodide solution containing 200 μg/ml boiled RNase, incubated at room temperature for 30 min in the dark, and analyzed by flow cytometry using a Becton Dickinson FACScan. Cell cycle was determined with the WEASELsoftware (WEHI Biotechnology Centre, Australia).

In vitro growth inhibition assays

Mouse RMS primary cell cultures were plated at 3×10^3 cells per well in a 96-well plate. After 24 h, ATM and VCR were added to the wells in a range of concentrations by serial dilution. siRNA against mouse *Prkci* was purchased from Dharmacon (LQ-040822-07, Lafayette, CO). Transient transfections were carried out using Lipofectamine 2000 (Invitrogen). Non-targeting siRNA (D-001810, Dharmacon) was used as control. After cells were incubated with ATM or siRNA for 72 h, cytotoxic effects were assayed using CellTiter 96® AQueous One Solution Cell Proliferation Assay system (Promega, Madison, WI) and SpectraMax M5 luminometer (Molecular Devices, Sunnyvale, CA). IC50 and C.I. were determined with CalcuSyn software (BIOSOFT, United Kingdom).

Anchorage-independent colony formation assay

Mouse RMS primary cell cultures were plated at 3×10^4 cells per well in a 6-well plate. The cells were transfected with siRNA (0, 10, 100 nM) before plating the top layer. 8 days after the cells were transfected with siRNA, colonies were fixed with methanol, treated with Giemsa stain and counted.

Invasion assay

Invasion assay was performed using the Culturex 96 well BME invasion assay kit (cat. no. 3455-096-K, R&D systems, Minneapolis, MN). Twenty-four hours prior to beginning assay, cells were starved in a serum-free medium. Top chambers were plated at a density of 5×10^4 cells/ well in 50 μl with DMEM and ATM at different concentration (0 to 500 μM). Bottom chambers were filled by 10%FBS/ DMEM or DMEM only as a negative control. The relative invasion was determined after 24 h of incubation using calcein–AM solution by reading the plate at 485 nm excitation and 520 nm emission wavelengths.

In vivo orthotopic allograft tumor growth inhibition studies

All experiments received prior approval from the OHSU Institutional Animal Use and Care Committee. 4–8 week old SHO-*Prkdc*^{scid}*Hr*^{hr} mice (Charles River Laboratories International, Inc., Wilmington, MA) were injected with 1×10^6 cells from mouse primary cell cultures into the cardiotoxin-preinjured gastrocnemius muscles. 3 days after injection, drug treatment started. 7 mice or 5 mice were used in control or each treatment group. Tumor volumes (cm^3) were measured 3-dimensionally with electronic calipers and calculated from formula ($\pi/6$) × length × width × height, assuming tumors to be spheroid.

Statistical analysis

All data are presented as mean ± sd. One-way ANOVA was used to determine statistical significance of expression analysis and in vitro assay. $P < 0.05$ was considered statistically significant.

Statistical analysis of *In vivo* orthotopic allograft tumor growth inhibition studies

Treatment groups were contrasted by pairwise comparisons between treatment groups with regard to mean tumor size using a repeated measures linear model with an auto-regressive covariance structure adjusted for day, treatment group and the interaction of day treatment and corrected for multiple testing using the Tukey method. Mean body weight by treatment groups were also compared using a repeated measures linear model with an auto-regressive covariance structure adjusted for day and treatment group and corrected for multiple testing using the Tukey method. The interaction of day treatment was not significant in the model.

Supplementary Material

Refer to Web version on PubMed Central for supplementary material.

Acknowledgments

This work was supported by NIH/NCI grant 1R01CA133229-04 and -05 awarded to CK, NIH/NCI grant 4R01CA081436-13 and the V Foundation for Cancer Research awarded to APF. Human tissue samples were provided by the Pediatric Cooperative Human Tissue Network which is funded by the National Cancer Institute. The Developmental Studies Hybridoma Bank is developed under the auspices of the NICHD and maintained by The University of Iowa, Iowa City, IA.

References

1. Anderson J, Gordon A, Pritchard-Jones K, Shipley J. Genes, chromosomes, and rhabdomyosarcoma. Genes Chromosomes Cancer. 1999 Dec; 26(4):275–85. [PubMed: 10534762]
2. Hayes-Jordan A, Andrassy R. Rhabdomyosarcoma in children. Curr Opin Pediatr. 2009 Jun; 21(3): 373–8. [PubMed: 19448544]
3. Arndt CA, Crist WM. Common musculoskeletal tumors of childhood and adolescence. N Engl J Med. 1999 Jul 29; 341(5):342–52. [PubMed: 10423470]
4. Breneman JC, Lyden E, Pappo AS, Link MP, Anderson JR, Parham DM, et al. Prognostic factors and clinical outcomes in children and adolescents with metastatic rhabdomyosarcoma--a report from the Intergroup Rhabdomyosarcoma Study IV. J Clin Oncol. 2003 Jan 1; 21(1):78–84. [PubMed: 12506174]
5. Wachtel M, Schafer BW. Targets for cancer therapy in childhood sarcomas. Cancer Treat Rev. 2010 Jun; 36(4):318–27. [PubMed: 20223596]
6. Mackay HJ, Twelves CJ. Targeting the protein kinase C family: are we there yet? Nat Rev Cancer. 2007 Jul; 7(7):554–62. [PubMed: 17585335]
7. Griner EM, Kazanietz MG. Protein kinase C and other diacylglycerol effectors in cancer. Nat Rev Cancer. 2007 Apr; 7(4):281–94. [PubMed: 17384583]
8. Fields AP, Murray NR. Protein kinase C isozymes as therapeutic targets for treatment of human cancers. Adv Enzyme Regul. 2008; 48:166–78. [PubMed: 18167314]
9. Ali AS, Ali S, El-Rayes BF, Philip PA, Sarkar FH. Exploitation of protein kinase C: a useful target for cancer therapy. Cancer Treat Rev. 2009 Feb; 35(1):1–8. [PubMed: 18778896]
10. Chen L, Burger RA, Zaunbrecher GM, Cheng H, Lincoln AJ, Mallarino MC, et al. Protein kinase C isoform expression and activity alter paclitaxel resistance in vitro. Gynecol Oncol. 1999 Feb; 72(2):171–9. [PubMed: 10021296]
11. Murray NR, Fields AP. Atypical protein kinase C iota protects human leukemia cells against drug-induced apoptosis. J Biol Chem. 1997 Oct 31; 272(44):27521–4. [PubMed: 9346882]
12. Svensson K, Larsson C. A protein kinase Cbeta inhibitor attenuates multidrug resistance of neuroblastoma cells. BMC Cancer. 2003 Mar 26.3:10. [PubMed: 12697075]
13. Fields AP, Regala RP. Protein kinase C iota: human oncogene, prognostic marker and therapeutic target. Pharmacol Res. 2007 Jun; 55(6):487–97. [PubMed: 17570678]

14. Regala RP, Weems C, Jamieson L, Khoor A, Edell ES, Lohse CM, et al. Atypical protein kinase C iota is an oncogene in human non-small cell lung cancer. Cancer Res. 2005 Oct 1; 65(19):8905–11. [PubMed: 16204062]
15. Ishiguro H, Akimoto K, Nagashima Y, Kojima Y, Sasaki T, Ishiguro-Imagawa Y, et al. aPKClambda/iota promotes growth of prostate cancer cells in an autocrine manner through transcriptional activation of interleukin-6. Proc Natl Acad Sci U S A. 2009 Sep 22; 106(38): 16369–74. [PubMed: 19805306]
16. Regala RP, Davis RK, Kunz A, Khoor A, Leitges M, Fields AP. Atypical protein kinase C{iota} is required for bronchioalveolar stem cell expansion and lung tumorigenesis. Cancer Res. 2009 Oct 1; 69(19):7603–11. [PubMed: 19738040]
17. Regala RP, Thompson EA, Fields AP. Atypical protein kinase C iota expression and aurothiomalate sensitivity in human lung cancer cells. Cancer Res. 2008 Jul 15; 68(14):5888–95. [PubMed: 18632643]
18. Regala RP, Weems C, Jamieson L, Copland JA, Thompson EA, Fields AP. Atypical protein kinase Ciota plays a critical role in human lung cancer cell growth and tumorigenicity. J Biol Chem. 2005 Sep 2; 280(35):31109–15. [PubMed: 15994303]
19. Scotti ML, Bamlet WR, Smyrk TC, Fields AP, Murray NR. Protein kinase Ciota is required for pancreatic cancer cell transformed growth and tumorigenesis. Cancer Res. 2010 Mar 1; 70(5): 2064–74. [PubMed: 20179210]
20. Win HY, Acevedo-Duncan M. Atypical protein kinase C phosphorylates IKKalphabeta in transformed non-malignant and malignant prostate cell survival. Cancer Lett. 2008 Nov 8; 270(2): 302–11. [PubMed: 18571841]
21. Win HY, Acevedo-Duncan M. Role of protein kinase C-iota in transformed non-malignant RWPE-1 cells and androgen-independent prostate carcinoma DU-145 cells. Cell Prolif. 2009 Apr; 42(2):182–94. [PubMed: 19243387]
22. Zhang L, Huang J, Yang N, Liang S, Barchetti A, Giannakakis A, et al. Integrative genomic analysis of protein kinase C (PKC) family identifies PKCiota as a biomarker and potential oncogene in ovarian carcinoma. Cancer Res. 2006 May 1; 66(9):4627–35. [PubMed: 16651413]
23. Murray NR, Jamieson L, Yu W, Zhang J, Gokmen-Polar Y, Sier D, et al. Protein kinase Ciota is required for Ras transformation and colon carcinogenesis in vivo. J Cell Biol. 2004 Mar 15; 164(6):797–802. [PubMed: 15024028]
24. Stallings-Mann M, Jamieson L, Regala RP, Weems C, Murray NR, Fields AP. A novel small-molecule inhibitor of protein kinase Ciota blocks transformed growth of non-small-cell lung cancer cells. Cancer Res. 2006 Feb 1; 66(3):1767–74. [PubMed: 16452237]
25. Erdogan E, Lamark T, Stallings-Mann M, Lee J, Pellecchia M, Thompson EA, et al. Aurothiomalate inhibits transformed growth by targeting the PB1 domain of protein kinase Ciota. J Biol Chem. 2006 Sep 22; 281(38):28450–9. [PubMed: 16861740]
26. Etienne-Manneville S, Hall A. Cell polarity: Par6, aPKC and cytoskeletal crosstalk. Curr Opin Cell Biol. 2003 Feb; 15(1):67–72. [PubMed: 12517706]
27. Murray NR, Kalari KR, Fields AP. Protein kinase Ciota expression and oncogenic signaling mechanisms in cancer. J Cell Physiol. 2011 Apr; 226(4):879–87. [PubMed: 20945390]
28. Cen L, Arnoczky KJ, Hsieh FC, Lin HJ, Qualman SJ, Yu S, et al. Phosphorylation profiles of protein kinases in alveolar and embryonal rhabdomyosarcoma. Mod Pathol. 2007 Sep; 20(9):936–46. [PubMed: 17585318]
29. Amstutz R, Wachtel M, Troxler H, Kleinert P, Ebauer M, Haneke T, et al. Phosphorylation regulates transcriptional activity of PAX3/FKHR and reveals novel therapeutic possibilities. Cancer Res. 2008 May 15; 68(10):3767–76. [PubMed: 18483260]
30. Fields AP, Frederick LA, Regala RP. Targeting the oncogenic protein kinase Ciota signalling pathway for the treatment of cancer. Biochem Soc Trans. 2007 Nov; 35(Pt 5):996–1000. [PubMed: 17956262]
31. Maroto B, Ye MB, von Lohneysen K, Schnelzer A, Knaus UG. P21-activated kinase is required for mitotic progression and regulates Plk1. Oncogene. 2008 Aug 21; 27(36):4900–8. [PubMed: 18427546]

32. Wittmann T, Bokoch GM, Waterman-Storer CM. Regulation of microtubule destabilizing activity of Op18/stathmin downstream of Rac1. J Biol Chem. 2004 Feb 13; 279(7):6196–203. [PubMed: 14645234]
33. Woodcock SA, Rushton HJ, Castaneda-Saucedo E, Myant K, White GR, Blyth K, et al. Tiam1-Rac signaling counteracts Eg5 during bipolar spindle assembly to facilitate chromosome congression. Curr Biol. 2010 Apr 13; 20(7):669–75. [PubMed: 20346677]
34. Blocka KL, Paulus HE, Furst DE. Clinical pharmacokinetics of oral and injectable gold compounds. Clin Pharmacokinet. 1986 Mar-Apr;11(2):133–43. [PubMed: 3082559]
35. Nelson RL. The comparative clinical pharmacology and pharmacokinetics of vindesine, vincristine, and vinblastine in human patients with cancer. Med Pediatr Oncol. 1982; 10(2):115–27. [PubMed: 7070351]
36. Houghton JA, Houghton PJ, Green AA. Chemotherapy of childhood rhabdomyosarcomas growing as xenografts in immune-deprived mice. Cancer Res. 1982 Feb; 42(2):535–9. [PubMed: 7034923]
37. Thompson J, George EO, Poquette CA, Cheshire PJ, Richmond LB, de Graaf SS, et al. Synergy of topotecan in combination with vincristine for treatment of pediatric solid tumor xenografts. Clin Cancer Res. 1999 Nov; 5(11):3617–31. [PubMed: 10589779]
38. Sorensen PH, Lynch JC, Qualman SJ, Tirabosco R, Lim JF, Maurer HM, et al. PAX3-FKHR and PAX7-FKHR gene fusions are prognostic indicators in alveolar rhabdomyosarcoma: a report from the children's oncology group. J Clin Oncol. 2002 Jun 1; 20(11):2672–9. [PubMed: 12039929]
39. Bouche M, Zappelli F, Polimeni M, Adamo S, Wetsel WC, Senni MI, et al. Rapid activation and down-regulation of protein kinase C alpha in 12-O-Tetradecanoylphorbol-13-acetate-induced differentiation of human rhabdomyosarcoma cells. Cell Growth Differ. 1995 Jul; 6(7):845–52. [PubMed: 7547506]
40. Germani A, Fusco C, Martinotti S, Musaro A, Molinaro M, Zani BM. TPA-induced differentiation of human rhabdomyosarcoma cells involves dephosphorylation and nuclear accumulation of mutant P53. Biochem Biophys Res Commun. 1994 Jul 15; 202(1):17–24. [PubMed: 8037710]
41. Liu LN, Dias P, Houghton PJ. Mutation of Thr115 in MyoD positively regulates function in murine fibroblasts and human rhabdomyosarcoma cells. Cell Growth Differ. 1998 Sep; 9(9):699–711. [PubMed: 9751114]
42. Thimmaiah KN, Easton JB, Houghton PJ. Protection from rapamycin-induced apoptosis by insulin-like growth factor-I is partially dependent on protein kinase C signaling. Cancer Res. 2010 Mar 1; 70(5):2000–9. [PubMed: 20179209]
43. Sundberg C, Thodeti CK, Kveiborg M, Larsson C, Parker P, Albrechtsen R, et al. Regulation of ADAM12 cell-surface expression by protein kinase C epsilon. J Biol Chem. 2004 Dec 3; 279(49): 51601–11. [PubMed: 15364951]
44. Limatola C, Barabino B, Nista A, Santoni A. Interleukin 1-beta-induced protein kinase C-zeta activation is mimicked by exogenous phospholipase D. Biochem J. 1997 Jan 15; 321(Pt 2):497–501. [PubMed: 9020886]
45. Jordan MA, Thrower D, Wilson L. Mechanism of inhibition of cell proliferation by Vinca alkaloids. Cancer Res. 1991 Apr 15; 51(8):2212–22. [PubMed: 2009540]
46. Tennyson GS, Burbach BJ, Lane BP. Reproductive potential of vincristine-treated multinucleate carcinoma cells. Cancer Treat Rep. 1983 Dec; 67(12):1113–4. [PubMed: 6652628]
47. Keller C, Arenkiel BR, Coffin CM, El-Bardeesy N, DePinho RA, Capecchi MR. Alveolar rhabdomyosarcomas in conditional Pax3:Fkhr mice: cooperativity of Ink4a/ARF and Trp53 loss of function. Genes Dev. 2004 Nov 1; 18(21):2614–26. [PubMed: 15489287]
48. Keller C, Hansen MS, Coffin CM, Capecchi MR. Pax3:Fkhr interferes with embryonic Pax3 and Pax7 function: implications for alveolar rhabdomyosarcoma cell of origin. Genes Dev. 2004 Nov 1; 18(21):2608–13. [PubMed: 15520281]
49. Nishijo K, Chen QR, Zhang L, McCleish AT, Rodriguez A, Cho MJ, et al. Credentialing a preclinical mouse model of alveolar rhabdomyosarcoma. Cancer Res. 2009 Apr 1; 69(7):2902–11. [PubMed: 19339268]
50. Rubin BP, Nishijo K, Chen HI, Yi X, Schuetze DP, Pal R, et al. Evidence for an unanticipated relationship between undifferentiated pleomorphic sarcoma and embryonal rhabdomyosarcoma. Cancer Cell. 2011 Feb 15; 19(2):177–91. [PubMed: 21316601]

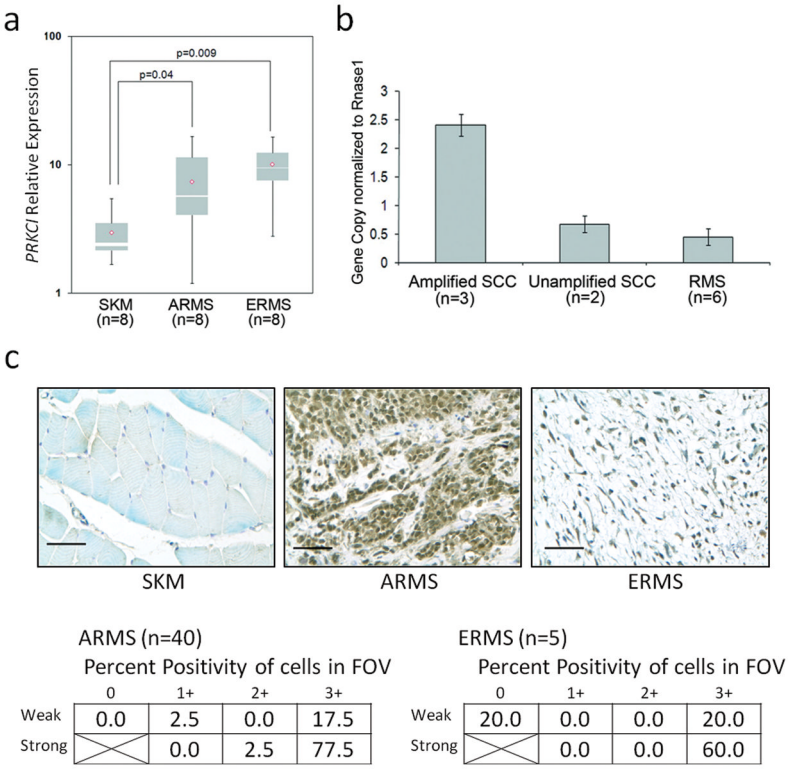

Figure 1.

Over-expression of PKCι in human RMS. (a) Quantitative RT-PCR shows that *PRKCI* is over-expressed in human ARMS and ERMS compared to normal skeletal muscle (2.5 and 3.4-fold respectively, $p<0.05$). (b) *PRKCI* DNA copy number does not account for the increased mRNA expression. (c) Protein expression of PKCι in human ARMS by immunohistochemistry (tumor cell specific). Size bar = 0.05 mm. Semi-quantitative scales are given in methods. Staining in normal skeletal muscle was rare.

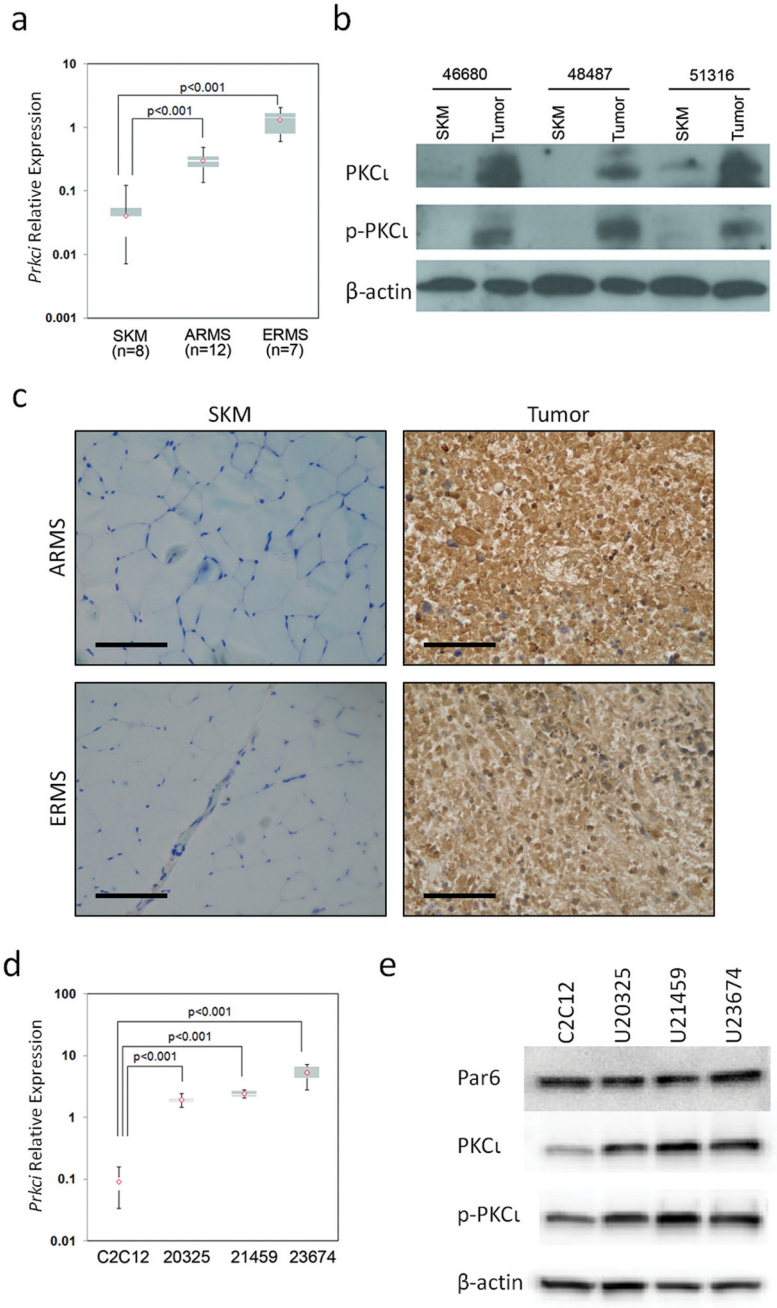

Figure 2.

Over-expression of PKCι in mouse ARMS. (a) Quantitative RT-PCR show *Prkci* is over-expressed in mouse ARMS and ERMS compared to normal skeletal muscle (7.5 and 33 fold respectively, p<0.001). (b) Immunoblotting for PKCι shows high expression and activation in mouse tumors compared to matched skeletal muscle. (c) PKCι immunohistochemistry of mouse tumors. Size bar = 0.05 mm. (d) *Prkci* is over-expressed in mouse ARMS primary cell cultures compared to mouse myoblast C2C12. (e) Immunoblots show Par6, PKCι and phospho-PKCι expression in mouse ARMS primary cell cultures. See Supplementary Figure S2 for full length blots of Figure 2e.

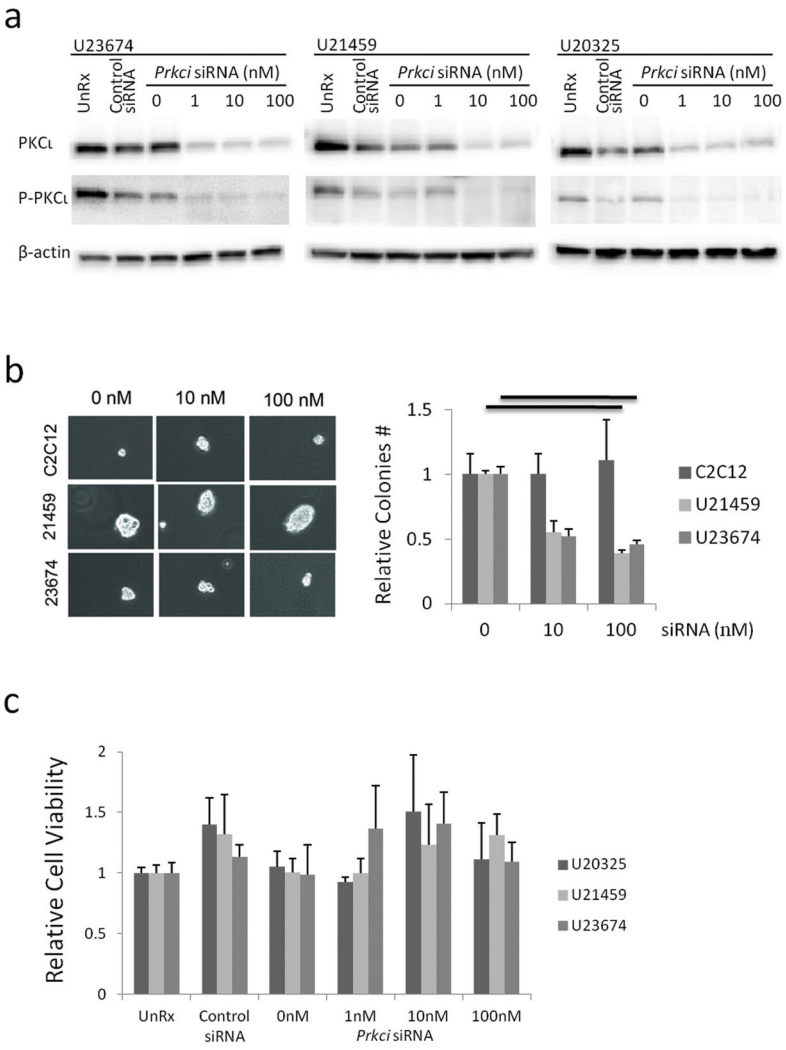

Figure 3.

In vitro knockdown of *Prkci* by siRNA. (a) Immunoblots of PKCι expression showing knockdown efficiency. (b) Anchorage-independent colony formation with increasing concentrations of *Prkci* siRNA. Mean ± SE were obtained from two independent experiments. Black line shows significant difference ($P<0.05$). (c) In vitro cell growth assay of mouse ARMS primary cell cultures treated with increasing concentrations of *Prkci* siRNA. See Supplementary Figure S3 for full length blots of Figure 3a.

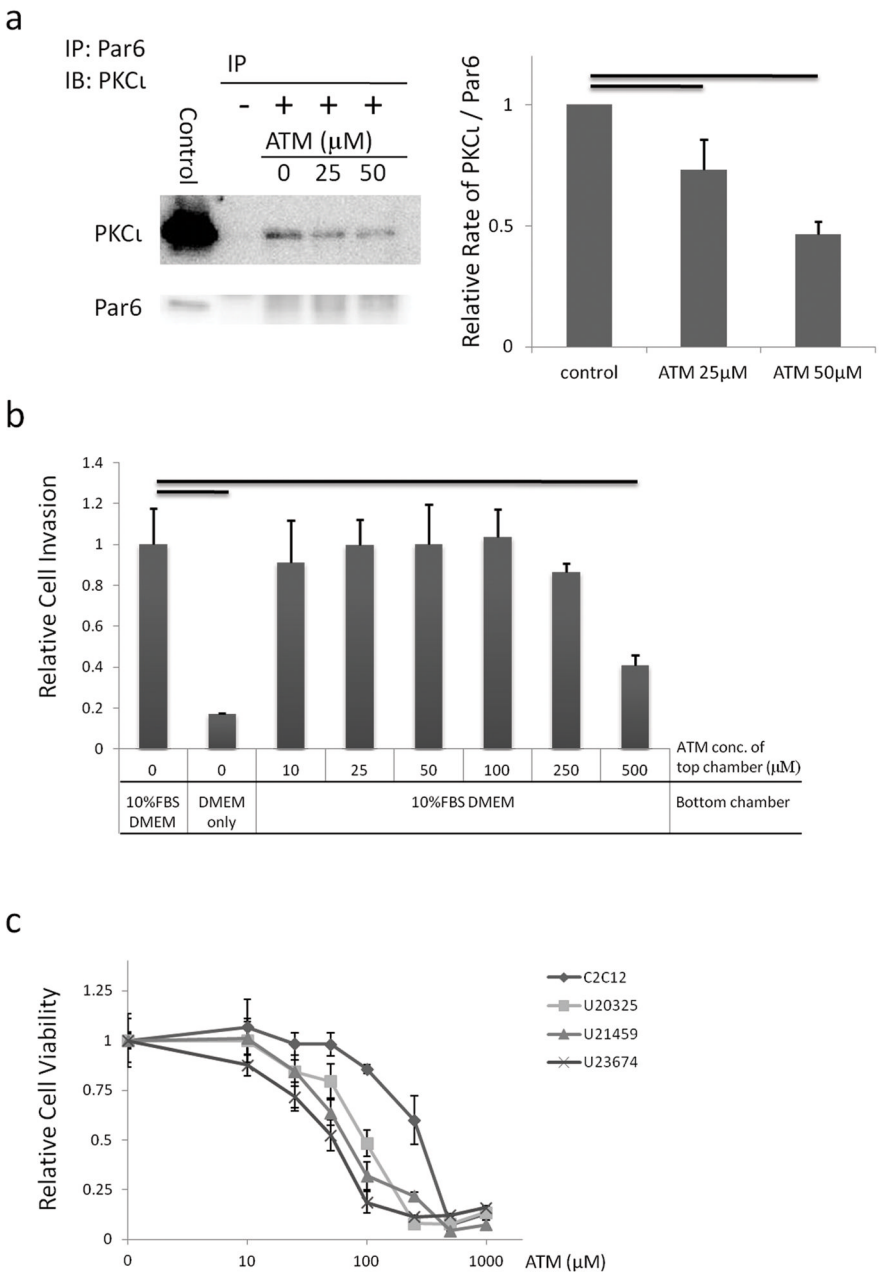

Figure 4.

Inhibition of PKCι by ATM. (a) Immunoprecipitation of PKCι and Par6 showing ATM inhibits interaction of PKCι and Par6. Numbers are relative rate of PKCι/Par6. Mean ± SE were obtained from three independent immunoblottings of immunoprecipitation. Black line shows significant difference ($P<0.05$). (b) Invasion potential of mouse ARMS primary cell cultures with increasing concentrations of ATM. Black line shows significant difference ($P<0.01$). (c) Cell growth assay for mouse primary cell cultures treated with increasing concentrations of ATM. See Supplementary Figure S4 for full length blots of Figure 4a.

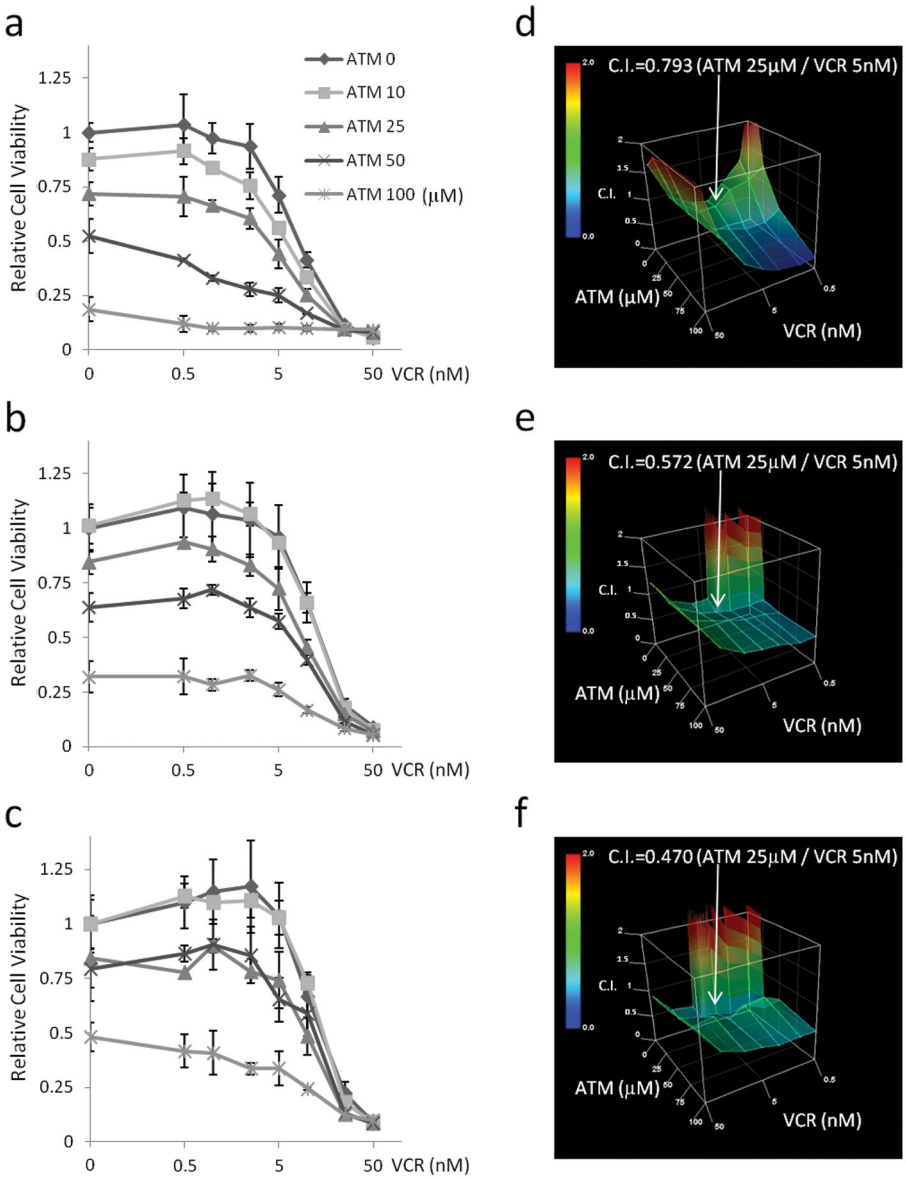

Figure 5.

Combination of ATM and VCR. (a–c) Cell growth assay for mouse primary cell cultures treated with ATM and VCR. (d–f) Combination index of ATM and VCR. (a, d) U23674. (b, e) U21459. (c, f) U20325.

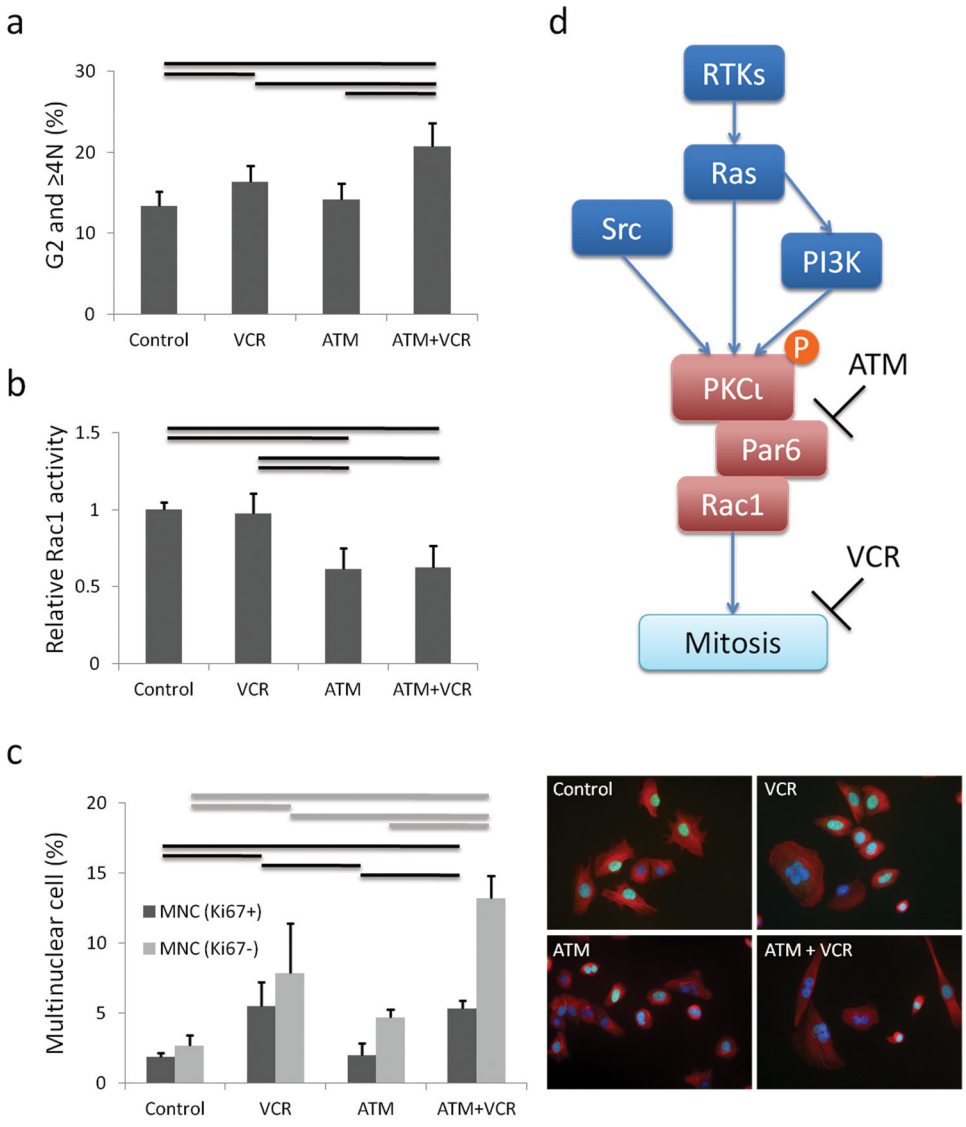

Figure 6.

Mechanism of synergy effects of ATM (25 μM) and VCR (5 nM) (a) Cell cycle analysis by FACS of cells treated with ATM and VCR. Mean ± SE were obtained from six independent experiments. Black line shows significant difference ($P<0.05$). (b) Rac1 activity is decreased by ATM, but not VCR. Mean ± SE were obtained from two independent experiments. Black line shows significant difference ($P<0.05$). (c) Immunofluorescence stain with Ki67, β-tubulin and DAPI showing non-proliferative multinuclear cells are increased by ATM and VCR. 200 cells were counted for each ICC experiment. Mean ± SE were obtained from three independent experiments. Black and gray lines show significant differences ($P<0.05$). (d) Schematic summary of ATM and VCR action. See Supplementary Figure S6 for representative ICC images corresponding to Figure 6c.

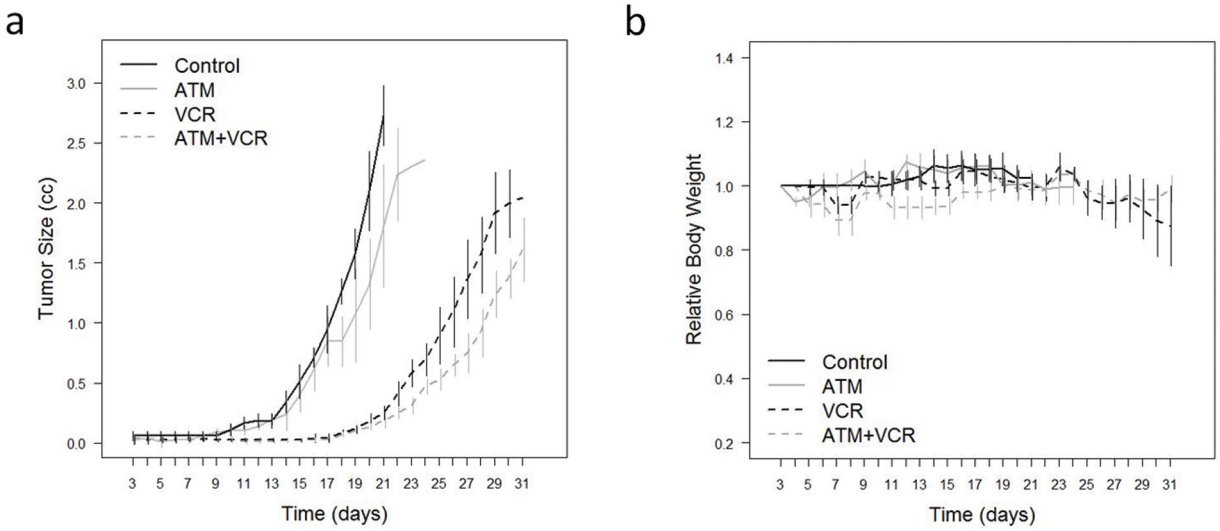

Figure 7.

Anti-tumor activity of combination with ATM and VCR against U23674 mouse ARMS primary cell culture orthotopic allograft in SHO mice. (a) Tumor size measured by caliper. Drugs were administered 3 days after tumor injection. Black line; control (n = 7), gray line; ATM 60 mg/kg daily i.m. (n = 5), black dotted line; VCR 1mg/kg weekly i.v. (n = 5), gray dotted line; ATM 60 mg/kg daily i.m. (n = 5), and VCR 1 mg/kg weekly i.v. (n = 5). (b) Change of body weight of mice treated with ATM and/or VCR. See Methods for statistical analysis in (a) and (b).